magnetization and H is the magnetic field strength, have been performed on crystals with a demagnetizing factor, N, of 0.1 to 0.3. The demagnetizing factor depends only on shape and determines the strength of the reverse field that appears inside a sample when it is magnetized; χ is limited by the demagnetizing effect to $1/N$. We therefore use long, thin samples with $N \approx 0.01$, and measure χ in a small alternating-current field of 8 A m^{-1}, compensating for the Earth's field with a pair of Helmholz coils.

Figure 1a shows that the real component $\chi'(T)$ measured perpendicular to the c-axis has a sharp peak at the magnetic transition with a maximum value of 49 ± 4. As the temperature decreases further, χ' increases to saturate near the demagnetizing-limited value $1/N = 77$. When the field is parallel to c, there is only a shoulder in $\chi'(T)$ at T_C and the value does not exceed 10. $\chi'(T)$ increases at lower temperature, reaching the demagnetizing limit $1/N = 66$ at 230 K.

Figure 1b shows the real and imaginary components, χ' and χ'', for the two directions in the vicinity of T_C, after correcting for the demagnetizing effect[4]. The $\chi_\perp'(T)$ peak at the magnetic transition is accompanied by a small peak in the $\chi_\perp''(T)$ component, but $\chi_\parallel'(T)$ barely exceeds 10 at T_C and $\chi_\parallel''(T)$ is zero within experimental error. There is no evident divergence at T_C. To see whether the observed non-divergence of the c-axis susceptibility could be related to pinning of domain walls, we applied a 50-Hz alternating-current bias field of 80 A m^{-1} to mobilize the walls. The form of χ' and χ'' did not change.

The susceptibility of a ferromagnet normally diverges as $|\epsilon|^{-\gamma}$, where $\epsilon = (T - T_C)/T_C$ and the critical exponent γ is 1.38 for isotropic spins (Heisenberg model) or 1.24 for extreme uniaxial anisotropy (Ising model). The presence of uniaxial dipolar anisotropy[5] should not prevent divergence at T_C.

Internal checks on the anomalous behaviour of $\chi_\parallel'(T)$ are provided by the divergence at lower temperatures in both directions and by the peak in $\chi_\perp(T)$. The susceptibility effectively reaches the demagnetizing-limited values at the spin-reorientation transition, but not at the Curie point. The sharp peak observed at T_C when the field is applied in the basal plane resembles the peak at the Néel point (at which anti-ferromagnetic materials become paramagnetic), T_N, of 230 K for terbium, where an in-plane helical structure is established[6] and χ' reaches a value of 8. When magnetized in-plane near T_C, where magnetocrystalline anisotropy is negligible, the susceptibility of gadolinium resembles that of a long-period helix rather than a true ferromagnet. When magnetized along c, there is a long-period sinusoidally modulated structure like that of erbium.

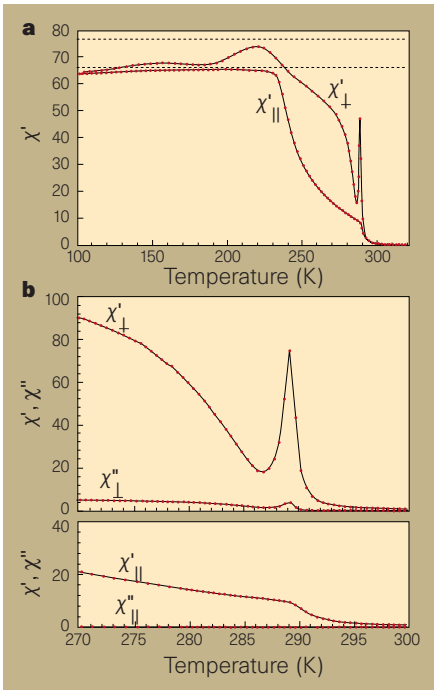

Figure 1 Magnetic susceptibility of a gadolinium crystal. **a,** Real and imaginary parts of the susceptibility measured with an alternating-current technique on long samples cut from a crystal of gadolinium with the field applied parallel (∥) and perpendicular (⊥) to the c-axis. The susceptibility is independent of frequency in the range 10 Hz to 1 kHz. The horizontal dotted lines indicate the saturation values expected for a divergent susceptibility, given the sample shape. **b,** Internal susceptibility of gadolinium in the vicinity of T_C, corrected for the demagnetizing effect caused by the sample shape.

The value of the exchange stabilization energy of the helix, $J(q_m) - J(0)$, may be estimated from the peak susceptibility using $\chi_{max} = \mu_0 N m^2 / \{S^2 [J(q_m) - J(0)]\}$ (ref. 7), where μ_0 is the permeability of free space, m is the atomic moment of gadolinium, $S = 7/2$, J is the exchange energy and q_m is the reduced wave vector in the c-direction; $\chi_{max} = 75$ gives $J(q_m) - J(0) = 0.013$ K. Extrapolating from the heavy rare-earth metals, where $J(q_m) - J(0) \approx q_m^4$, we estimate that $q_m = 0.029$ Å^{-1}; the corresponding wavelength, λ_m, is 70 Å.

Examination of gadolinium close to T_C, using techniques to observe the long-period modulation directly, may confirm that gadolinium is not really ferromagnetic.

J. M. D. Coey, V. Skumryev, K. Gallagher
Physics Department, Trinity College, Dublin 2, Ireland

1. Belov, K. P. & Pedko, A. L. *Zh. Eksp. Teor. Fiz.* **47,** 87 (1962). (English transl., *Sov. Phys. JETP* **15,** 62–64 (1962).
2. Cable, J. W. & Wollan, E. O. *Phys. Rev.* **165,** 733–734 (1968).
3. Dan'kov, S. Y., Tishin, A. M., Pecharsky, V. K. & Gschneider, K. A. Jr *Phys. Rev. B* **57,** 3478–3489 (1998).
4. Chen, D.-X. & Sanchez, A. *J. Appl. Phys.* **70,** 5463–5477 (1991).
5. Geldart, D. J. W., Hargraves, P., Fujiki, N. M. & Dunlap, R. A. *Phys. Rev. Lett.* **62,** 2728–2731 (1989).
6. del Moral, A. & Lee, E. W. *J. Phys. F* **4,** 280–290 (1974).
7. Kitano, Y. & Nagamia, T. *Prog. Theor. Phys.* **31,** 1–37 (1964).

Physiology

Warm feet promote the rapid onset of sleep

Even healthy people occasionally have difficulty falling asleep. Psychological relaxation techniques, hot baths, soothing infusions of plant extracts, melatonin and conventional hypnotics are all invoked in the search for a good night's sleep. Here we show that the degree of dilation of blood vessels in the skin of the hands and feet, which increases heat loss at these extremities, is the best physiological predictor for the rapid onset of sleep. Our findings provide further insight into the thermoregulatory cascade of events that precede the initiation of sleep[1].

Our analysis combines data from two intervention studies designed to induce phase shifts in the circadian pacemaker[2,3]. Healthy young men were given melatonin, bright light, or both, in the evening ($n = 8$), or a large carbohydrate-rich meal in either the morning or the evening ($n = 10$). These manipulations had different thermoregulatory effects and so gave a broad variance, enabling us to extract the best predictor variables for the latency of sleep onset.

Subjects lay in bed under controlled conditions (lighting less than 8 lux; 22 °C), taking small snacks of constant caloric value every hour during wakefulness. The latency of sleep onset was defined as the time between lights out (24:00) and the first occurrence of stage 2 in the sleep EEG recordings. Heart rate, core body temperature (rectal) and proximal (combined infraclavicular, thigh, stomach, forehead) and distal (combined hands and feet) skin temperatures were continuously measured[4] (and later collapsed into 30-min bins). Sleepiness was rated[2] every 30 min and saliva was collected for melatonin assay[5]. We calculated the distal–proximal temperature gradient (DPG), a measure of blood flow in distal skin regions (efficiently regulated by artereovenous anastomoses)[6] that provides an indirect index of distal heat loss.

By using a multiple regression model for repeated measures, with the latency of sleep onset as the dependent variable ($n = 18$ subjects, 144 data points; between-subjects differences taken into account), we found the highest correlation with the DPG averaged over the three data points between 22:30 and 24:00 ($r = -0.47$, $P < 0.0001$). Thus, the greater the distal vasodilation in the late evening, the shorter was the time taken to fall asleep. We found that correlations were weaker with subjective sleepiness ratings ($r = -0.33$, $P < 0.0001$), core body temperature ($r = 0.26$, $P < 0.005$), melatonin ($r = -0.15$, n.s.; after excluding the melatonin intervention data), rate of change of core body temperature ($r = -0.05$, n.s.) and heart rate ($r = 0.05$, n.s.).

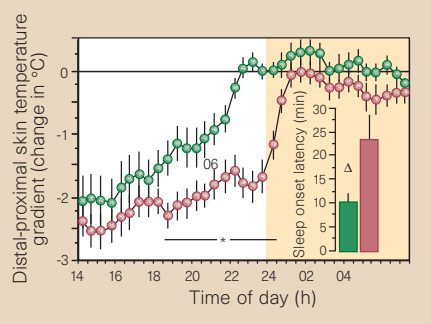

Figure 1 Time course of the distal–proximal skin-temperature gradient (DPG). The gradient is shown from 14:00 to 7:30 for observations with the most negative DPG values between 22:30 and 24:00 (large vasoconstriction before lights out at 24:00; pink symbols), compared with the time course of the most positive DPG values (large vasodilation before lights out; green symbols) (mean ± s.e.m., $n = 18$; asterisk indicates significant differences between data points; $P < 0.05$, Bonferroni-adjusted least significant differences). The shaded area indicates the lights-out period. These two extreme patterns were selected after the mean of the three DPG values between 22:30 and lights out at 24:00 had been rank ordered out of 8 observations for each subject. Sleep onset latency (inset) is significantly shorter when subjects were most vasodilated (green bar) before lights out (triangle indicates significant differences; paired t-test, $P < 0.001$).

In a backward stepwise regression analysis among all predictor variables, only DPG contributed significantly to the model; that is, vasodilation of distal skin regions was the best predictor of the body's readiness for sleep (Fig. 1). Because interventions such as light or large carbohydrate-rich meals differentially manipulated the independent variables, the effect on the dependent variable showed that the link between distal vasodilation and the ability to fall asleep is functional, not just correlative.

The circadian clock prepares the thermoregulatory system for vasodilation to begin in the early evening as sleepiness increases, followed by a drop in core body temperature. Even lying down increases sleepiness by redistributing heat in the body from the core to the periphery[7]. Turning out the light is a complex cognitive and physiological signal that also leads to vasodilation[4]. There is a tight correlation between the timing of the endogenous increase in melatonin in the evening and vasodilation, an effect that is mimicked by pharmacological doses of melatonin[4,7]. Before bedtime, then, many overlapping events orchestrate the thermoregulatory overture.

We would predict that classical hypnotics[8] and other sleep-inducing aids all cause dilation of distal blood vessels and heat loss before the onset of sleep. A hot-water bottle at the feet, while not acting on mechanisms in the central nervous system that underly the regulation of sleep, can rapidly induce vasodilation. The resulting heat loss is most efficient when the ambient temperature is cool[9]. Some sleep disorders (particularly those associated with ageing and somatic illness[10]) may be secondary to an inability to vasodilate and prepare the body for sleep.

Kurt Kräuchi, Christian Cajochen, Esther Werth, Anna Wirz-Justice
Chronobiology and Sleep Laboratory, Psychiatric University Clinic, Wilhelm Klein-Strasse 27, 4025 Basel, Switzerland
e-mail: kurt.kraeuchi@pukbasel.ch

1. Campbell, S. S. & Broughton, R. J. *Chronobiol. Int.* **11,** 126–131 (1994).
2. Cajochen, C., Kräuchi, K., Danilenko, K. V. & Wirz-Justice, A. *J. Sleep Res.* **7,** 145–157 (1998).
3. Wirz-Justice, A. *et al. J. Sleep Res.* **7** (suppl. 2), 308 (1998).
4. Kräuchi, K., Cajochen, C., Möri, D., Hetsch, C. & Wirz-Justice, A. *Am. J. Physiol.* **272,** R1178–R1188 (1997).
5. Weber, J. M., Unger, I., Wirz-Justice, A. & Schwander, J. C. *J. Sleep Res.* **7** (suppl. 2), 302 (1998).
6. Rubinstein, E. H. & Sessler, D. I. *Anesthesiology* **73,** 541–545 (1990).
7. Kräuchi, K., Cajochen, C. & Wirz-Justice, A. in *Circadian Clocks and Entrainment* (eds Honma, K. I. & Honma, S.) 131–146 (Hokkaido Univ. Press, Sapporo, 1998).
8. Gilbert, S. S., van den Heuvel, C. J. & Dawson, D. *J. Physiol. (Lond.)* **514,** 905–914 (1999).
9. Aschoff, J. *Wien. Med. Woch.* **19/20,** 404–409 (1958).
10. Foley, D. J. *et al. Sleep* **18,** 425–432 (1995).

Biological motors

Connecting stalks in V-type ATPase

In all organisms, adenosine triphosphate (ATP) provides metabolic energy for driving energy-dependent processes. It is synthesized and/or utilized by enzymes known as F-type and V-type ATPases, which are small rotary motors[1,2]. Both types consist of a headpiece, F_1 or V_1, respectively, which is connected by a stalk region to the membrane-bound part, F_O or V_O. Electron microscopic analysis of negatively stained particles has revealed a peripheral stalk, or stator, between V_1 and V_O of the V-type (Na^+)ATPase of the thermophilic bacterium *Clostridium fervidus*[3,4], like that in F-type ATPases[5,6]. We have analysed many more particles and now present a more complete structure of the V-type ATPase stator moiety.

A central stalk in the ATPase rotates within a ring of three α- and three β-subunits in F_1 (refs 7, 8), or three A and three B subunits in V_1, in discrete steps of 120°. At the F_O/V_O end, the central stalk is connected to a ring of c subunits in the membrane. These subunits rotate against other subunits of F_O and V_O, allowing ion translocation at the interface[2]. A stator structure in the form of additional connections between F_1/V_1 and F_O/V_O must presumably be present to prevent futile rotation of the α3β3 and A3B3 headpiece[2].

We classified a set of 7,500 molecular projections of detergent-solubilized, negatively stained V_1V_O, and found a few preferential orientations in which V_1 has either two or three lobes. In about 28% of all views, there are three connections between V_1 and V_O, but in the rest either one (33%) or both (39%) of the peripheral connections appear to be missing. The three connections are well separated in the bilobed views (Fig. 1a). In the classes with trilobed views, the left connection is less well resolved because it is closer to the central stalk and overlaps more with V_1 (Fig. 1b). The two peripheral connections are each attached to an oval-shaped area of density on top of V_1. In some other classes (not shown), one of the oval densities is absent, which correlates with the loss of a peripheral connection. We conclude that the intact V-type ATPase has a central stalk and two stator connections (Fig. 1c, d). Likely candidates for the stators are the bacterial V-type subunits I, E and F, several copies of which are present.

The discovery of the second stator raises several points. First, although it has been suggested that there may be two stators[9], this feature has not been observed before. This could be because the intact structure is easily damaged on preparation, which can be detected only by classifying large sets of projections. The two stators may be unique for V-type ATPases because, in the stalk region of F-type ATPases, only the b subunit is present in two copies, as a dimer[10], participating in one stator. It is harder to visualize the stator(s) in F-type ATPase by electron microscopy because the stalk region is much shorter than in V-type ATPase[8].

Second, there could be more than two stators: three would match the three-fold symmetrical ring of the six large subunits

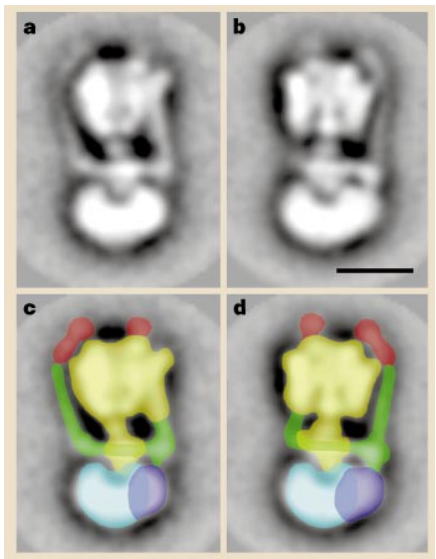

Figure 1 Electron microscopy images of V_1V_0 in side view. **a, b,** Views obtained by classification: **a,** bilobed view[3]; **b,** trilobed view. **c, d,** Model of the arrangement of the stator moiety (green) and its attachment to the V_1 headpiece (yellow) by the two oval densities (red). The view in **d** shows a larger additional density (dark blue) of V_0 on the right side than that in **c**. The stator moiety is attached to this additional density, which represents the static part of V_0. The view in **d** is obtained by rotating **c** about 30° backwards on the left. Scale bar, 100 Å.